

# Rheological and Extrusion Characteristics of Glass Fiber-Reinforced Polycarbonate

B. ANDERS KNUTSSON\* and JAMES L. WHITE, *Polymer Engineering, University of Tennessee, Knoxville, Tennessee 37916*, and  
KENT B. ABBAS, *Telefon AB LM Ericsson, Stockholm, Sweden*

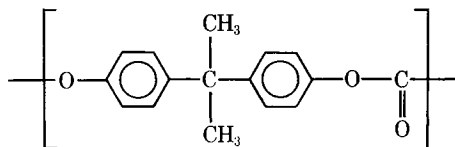
## Synopsis

An experimental investigation of the rheological properties of glass fiber-reinforced polycarbonate melts and the extrusion of such compounds through capillary and slit dies is presented. The viscosity-shear rate function seems independent of instrument for cone-plate and capillary investigations. The presence of fibers increases the level of the viscosity. Normal stresses at fixed shear stress are also increased by the presence of fibers. The extrudate swell is decreased by the presence of fibers and surface roughness is increased. Fiber orientation increases and surface roughness decreases with increasing extrusion rate.

## INTRODUCTION

Fiber-reinforced polymers are becoming increasingly important. This has led to growing interest in the flow characteristics of fiber-reinforced polymer melts.<sup>1-7</sup> Early studies generally emphasized measurement of the shear viscosity function in extrusion apparatus and have been limited largely to polyolefins and polystyrene<sup>1-5,7</sup> melts, though one study of polyethylene terephthalate<sup>6</sup> has appeared. Indeed only two experimental studies have appeared which contain rheological measurements of fiber-reinforced polymer melts in other instruments and for properties other than the shear viscosity.<sup>4,7</sup> Other types of investigations of flow behavior seem limited as well. Only two publications<sup>7,8</sup> seriously investigate the problem of fiber damage in flow. There are more extensive investigations of fiber motions and orientation in the flow of thermoplastics,<sup>6,9-11</sup> thermosets,<sup>12,13</sup> Newtonian model fluids,<sup>14,15</sup> and polymer solutions.<sup>16</sup>

It is our purpose in this article to consider the influence of glass fibers on the flow characteristics of polycarbonate:



This should be of interest because polycarbonate molecules which contain a *p*-linked benzene ring in their backbone are more rigid. While some studies of the rheological properties of polycarbonate have appeared elsewhere,<sup>17-20</sup> there has been none for fiber-reinforced polycarbonate. In this article we will investigate the influence of glass fibers on both the shear viscosity and principal normal stress difference as well as on extrudate character.

\* Permanent address: Telefon AB LM Ericsson, Kristianstad, Sweden.

TABLE I  
Systems Investigated for Glass Fiber-Reinforced Polycarbonate

Material	Supplier	Glass content, % (by weight)	$\bar{M}_w \times 10^{-3}$	$\bar{M}_w/\bar{M}_n$	Note
Makrolon 2805	Bayer AG	0	29.3	2.44	
Makrolon 6555	Bayer AG	0	28.9	2.43	Contains flame retardant
Makrolon 9410	Bayer AG	10			Contains flame retardant
Makrolon 8324	Bayer AG	20	30.4	2.41	
Makrolon 8035	Bayer AG	30	30.7	2.34	
Makrolon 8344	Bayer AG	40	27.9	2.51	

## EXPERIMENTAL

### Materials

The polycarbonates and the glass fiber-reinforced polycarbonate compounds were produced by Bayer AG of West Germany. The systems investigated are summarized in Table I.

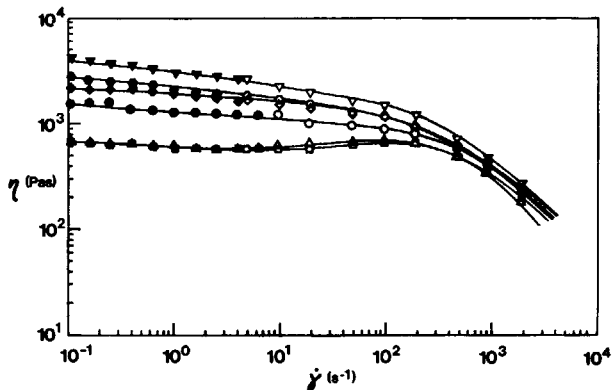


Fig. 1. Shear viscosity vs. shear rate for polycarbonates and fiber filled polycarbonates.  $T = 290^\circ\text{C}$ . Glass fibers: Makrolon 2805,  $\blacksquare$  = 0%; Makrolon 6555,  $\blacktriangle$  = 0%; Makrolon 9410,  $\bullet$  = 10%; Makrolon 8324,  $\blacktriangledown$  = 20%; Makrolon 8035,  $\blacklozenge$  = 30%; Makrolon 8344,  $\bullet$  = 40%.

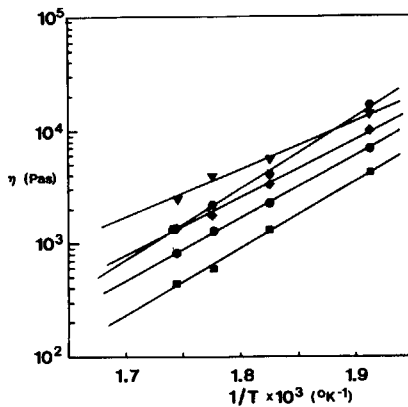


Fig. 2. Zero viscosity vs. reciprocal temperature (same symbols as Fig. 1).

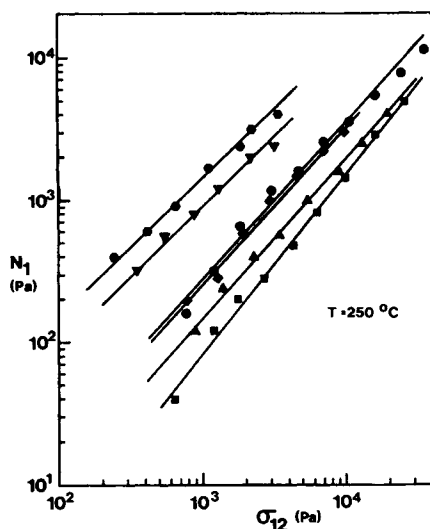


Fig. 3. Principal normal stress difference vs. shear stress (same symbols as Fig. 1).  $T = 250^{\circ}\text{C}$ .

Molecular weight distributions of the polycarbonates were measured in a Waters Associates gel permeation chromatography (GPC) model 200 by the method of Abbas.<sup>21</sup> The experimental conditions were as follows: solvent, methylene chloride, temperature,  $25^{\circ}\text{C}$ ; columns,  $10^6$ ,  $10^5$ ,  $10^4$ ,  $10^3$  Å; flow rate, 1 ml/min; sample concentration 2 g/l; injection time, 2 min, and sensitivity;  $8\times$ . Weight-average molecular weights,  $M_w$ , and ratios of weight-average to number-average molecular weight  $M_w/M_n$  are also summarized in Table I.

### Rheological Measurements

Polycarbonate pellets were dried at  $120^{\circ}\text{C}$  for a period of at least 12 h in an oven before proceeding. The pellets were compression molded at  $290^{\circ}\text{C}$ . Shear viscosities and principal normal stress differences were measured in a Rheometrics Mechanical Spectrometer. The sheets were predried in the same manner as the pellets before testing. All measurements were carried out in the cone-plate mode using a radius,  $R$ , of 12.5 mm and a cone angle,  $\alpha$ , of  $4^{\circ}$ . The shear stress,  $\sigma_{12}$ , and principal normal stress difference,  $N_1$ , were determined from the torque and thrust. The measurements in the cone-plate geometry were limited to shear rates below  $10\text{ sec}^{-1}$  for unreinforced polycarbonate and slightly less for the re-

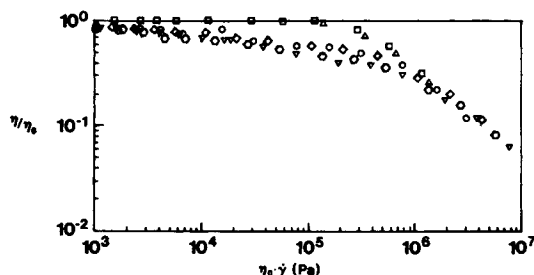


Fig. 4. Reduced viscosity,  $\eta/\eta_0$  curve for polycarbonate systems vs.  $\eta_0\dot{\gamma}$ .

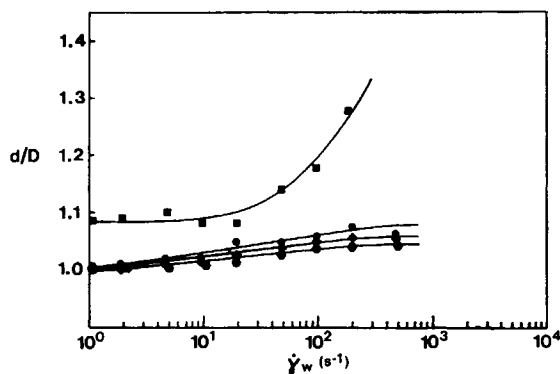


Fig. 5. Extrudate swell vs. wall shear rate (same symbols as Fig. 1).  $T = 290^{\circ}\text{C}$ .

inforced grades, owing to flow instabilities at the outer edge of the instrument. Capillary measurements were carried out in an Instron capillary rheometer using a series of dies with diameter of 1.47 mm and length/diameter or  $L/D$  ratios of 5, 10, 20, 30, and 40. The shear stress was obtained from a Bagley plot<sup>22</sup> of total pressure versus die  $L/D$ . The shear rate  $\dot{\gamma}_w$  at the die wall was determined by the Weissenberg relation,<sup>4,7,23</sup> where  $O$  is the extrusion rate.

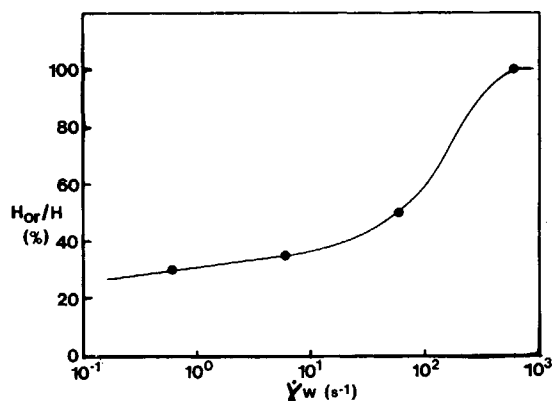


Fig. 6. Orientation ratio ( $H_{or}/H$ ) vs. wall shear rate (same symbols as Fig. 1).

TABLE II  
Fiber Length Distribution before and after Extrusion

Material	Glass content, %	Shear rate									
		$\bar{L}_n$		$\bar{L}_w$		$\bar{L}_z$		$\bar{L}_w/\bar{L}_n$		Standard deviation	
		0	1922	0	1922	0	1922	0	1922	0	1922
Makrolon 9410	10	454	392	603	509	738	591	1.33	1.30	262	216
Makrolon 8324	20	312	288	439	377	569	435	1.41	1.31	200	161
Makrolon 8035	30	124	96	172	131	221	171	1.39	1.37	78	58
Makrolon 8344	40	261	209	365	283	456	363	1.40	1.35	166	125

Viscosity measurements were carried out at 290°C in both instruments and also at 250, 275, and 300°C in the Mechanical Spectrometer. Principal normal stress differences were too small to measure accurately at the higher temperatures. We obtained our  $N_1$  data at 250°C.

### Extrusion through Slit and Capillary Dies

Extrusion experiments were carried out using a slit die of dimensions  $1.0 \times 6.0 \times 25$  mm for fiber orientation studies and capillary dies with diameters of 1.47 mm and  $L/D$  of 20 for surface morphological studies and  $L/D$  of 40 for extrudate swell studies. The polycarbonates were dried as previously indicated. The melt was fed into the dies from the reservoir of an Instron capillary rheometer.

The extrusion pressures were monitored and extrudate shapes were characterized. The extrudates were cross sectioned and examined using a scanning electron microscope (AMR model 900, Advanced Metals Research Corp., Burlington, MA). The orientations of fibers were determined at various positions in the cross section as a function of extrusion rate.

The shear rate at the die wall for a slit die can be obtained from the expression<sup>23,24</sup>

$$\dot{\gamma}_w = \left( \frac{2n'' + 1}{3n''} \right) \frac{6Q}{Hw} \quad (1a)$$

where

$$n'' = \frac{d \log (b \Delta p_d / L)}{d \log (6Q / Hw)} \quad (1b)$$

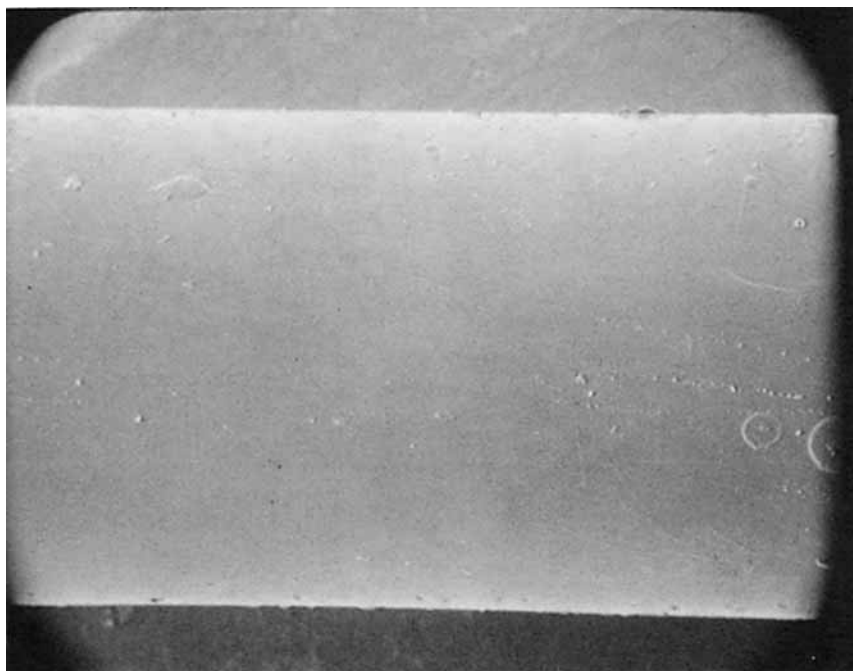
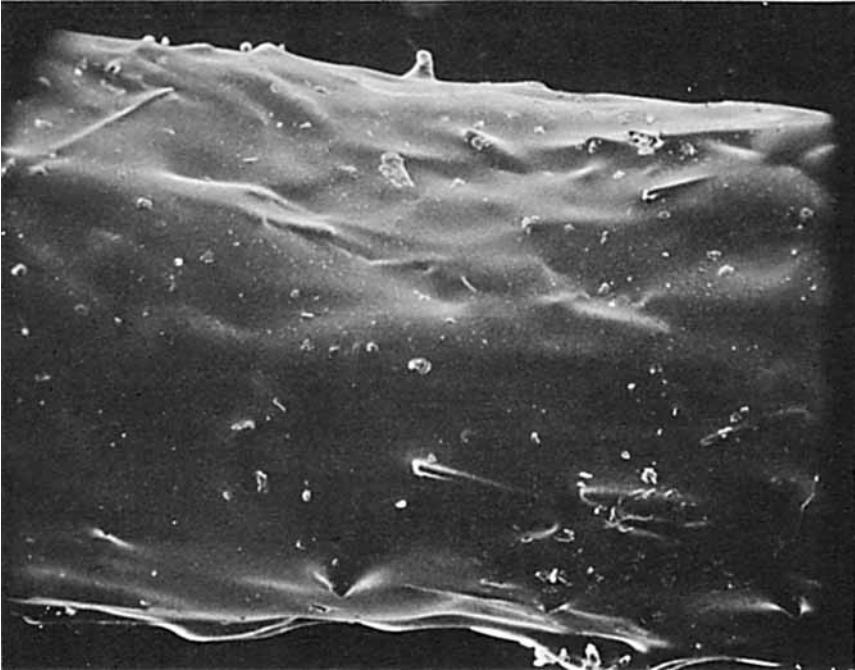


Fig. 7. SEM photomicrographs of polycarbonate extrudates.  $\dot{\gamma} = 19 \text{ s}^{-1}$ .

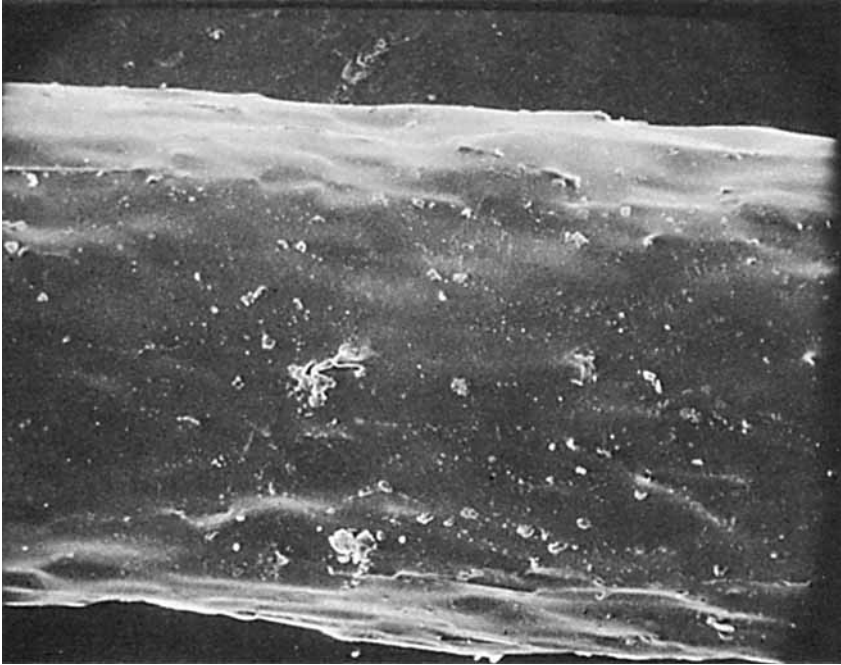


(a)



(b)

Fig. 8. SEM photomicrographs of 10% glass fiber/polycarbonate extrudates.  $\dot{\gamma}$ : (a), 19; (b), 192; (c), 1922 s<sup>-1</sup>.



(c)

Fig. 8. (Continued from previous page.)

Here  $Q$  is the extrusion rate,  $\Delta p_d$  the pressure loss within the die,  $w$  the die width, and  $H$  the thickness of the channel.

The extrusion experiments were all carried out at 290°C.

### Fiber Length Distribution

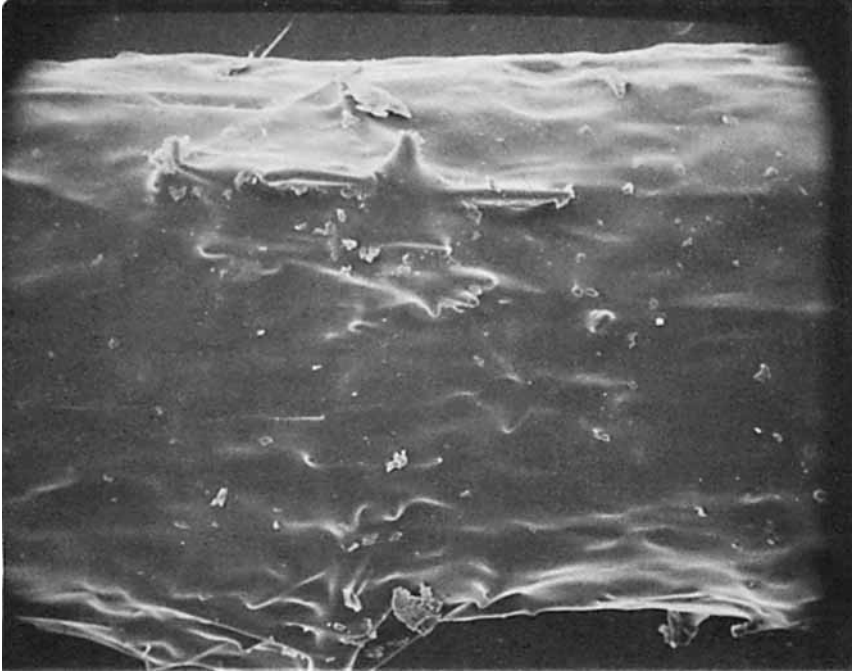
The polycarbonate was dissolved away from the compounds by using methylene chloride. The fibers were studied in an Orthoplan microscope (model 758962, Leitz Wetzlar).

We represent the fiber length distribution in terms of the moments

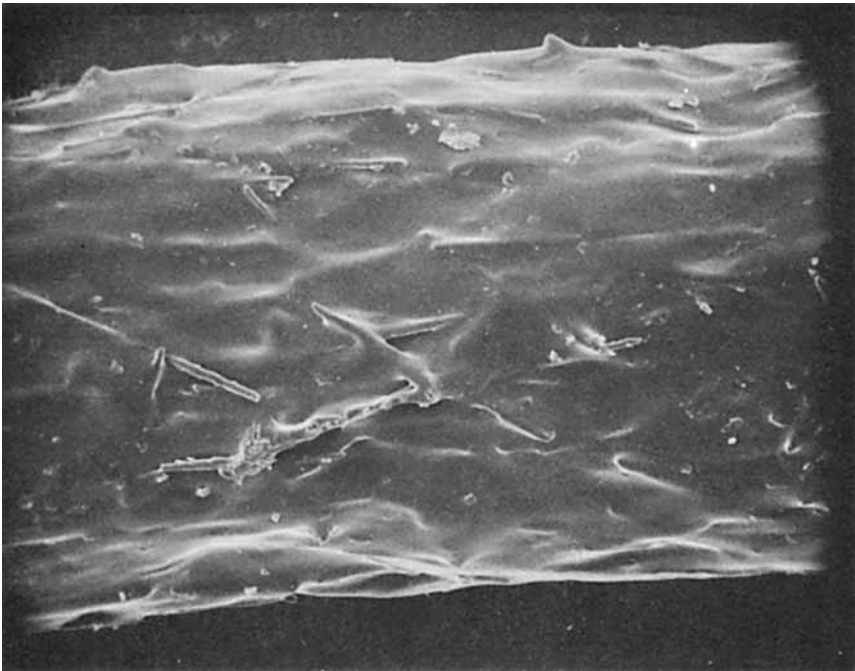
$$\bar{L}_n = \frac{\sum_i N_i L_i}{\sum_i N_i} \quad (2a)$$

$$\bar{L}_w = \frac{\sum_i N_i L_i^2}{\sum_i N_i L_i} \quad (2b)$$

$$\bar{L}_z = \frac{\sum_i N_i L_i^3}{\sum_i N_i L_i^2} \quad (2c)$$



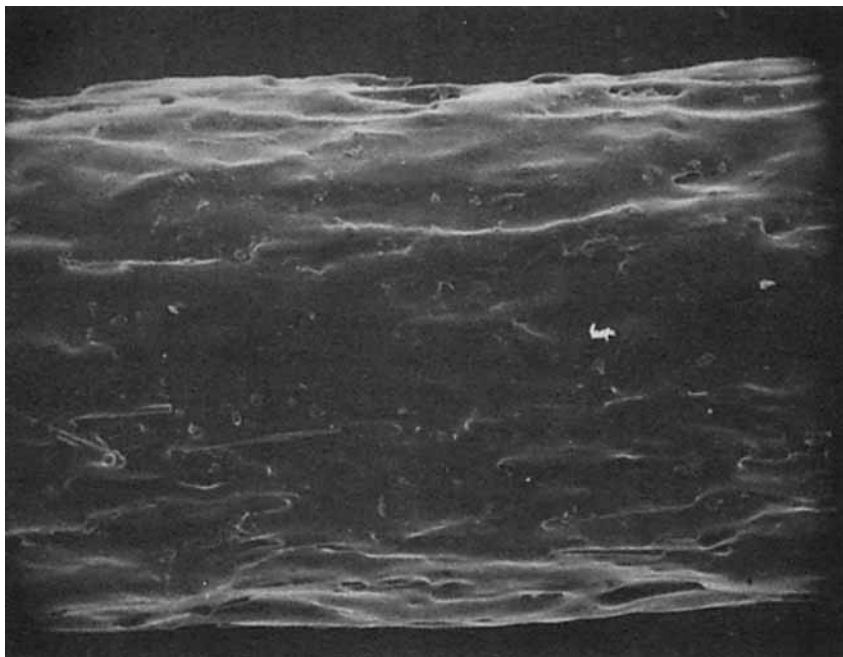
(a)



(b)

Fig. 9. SEM photomicrographs of 20% glass fiber/polycarbonate extrudates.  $\dot{\gamma}$ : (a), 19; (b), 192; (c), 1922  $s^{-1}$ .





(c)

Fig. 9. (Continued from previous page.)

and the polydispersity as  $\bar{L}_w/\bar{L}_n$ . The standard deviation was also determined.

The fiber length distributions were measured for virgin material and after extrusion through a capillary die with diameter of 1.47 mm,  $L/D$  of 20 at a temperature of 290°C and an apparent shear rate of 1922  $\text{sec}^{-1}$ .

## RHEOLOGICAL PROPERTIES

### Results

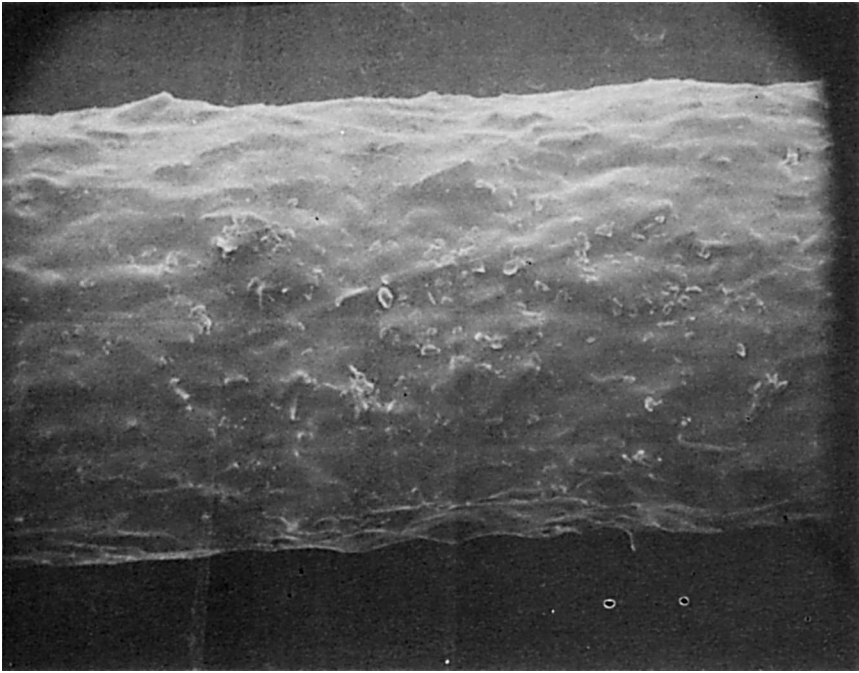
#### *Viscosity*

Shear viscosity measurements on the melts and the compounds investigated at 290°C are summarized in Figure 1. The data for the cone-plate and capillary instruments agree. The zero shear viscosities are of the order  $10^3$  Pa-sec, and at shear rates of 150  $\text{sec}^{-1}$  begin to decrease with increase in shear rate. Generally, the fiber-reinforced melts exhibit higher viscosities than the unfilled melt, although there is not a monotonic increase with loading level.

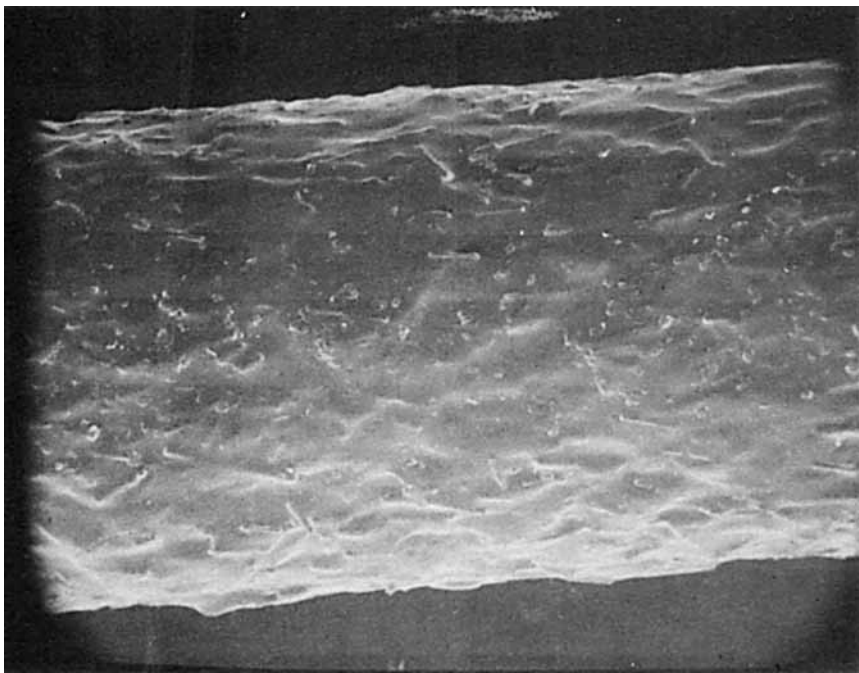
The temperature dependence of the viscosity data is shown in Figure 2. The viscosity decreases with increasing temperature.

#### *Principal Normal Stress Difference*

In Figure 3, we plot the principal normal stress difference,  $N_1$ , as a function of shear stress  $\sigma_{12}$ . Plots were made in this manner following the work of Han<sup>25</sup> and Oda, White, and Clark,<sup>26</sup> who show them to be independent of temperature for polystyrenes and polyolefins. Czarnecki and White<sup>7</sup> found this a useful

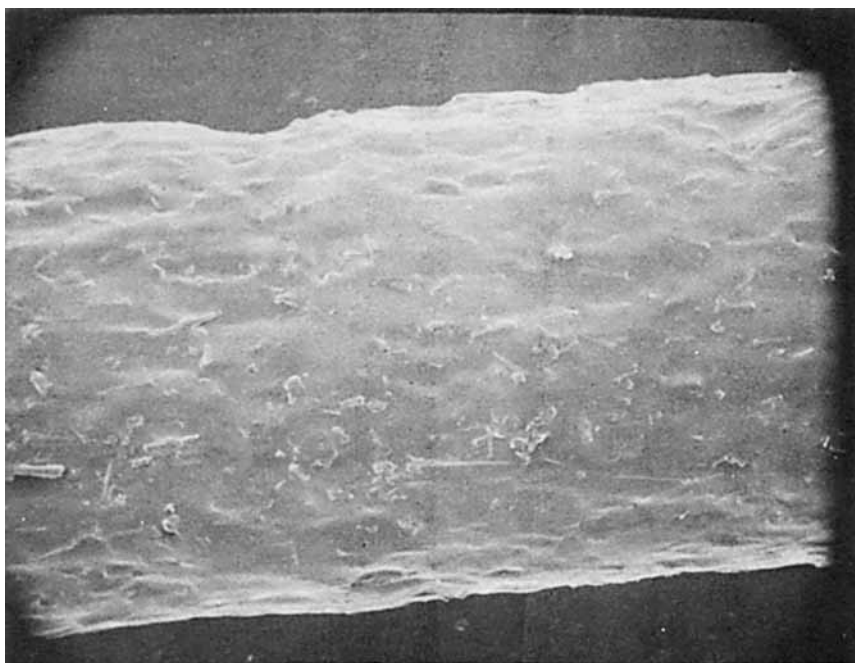


(a)



(b)

Fig. 10. SEM photomicrographs of 30% glass fiber/polycarbonate extrudates.  $\dot{\gamma}$ : (a), 19; (b), 192; (c), 1922 s<sup>-1</sup>.



(c)

Fig. 10. (Continued from previous page.)

manner of showing the effects of various types of fibers on  $N_1$  for filled polystyrene melts. We see that the values of  $N_1$  at fixed  $\sigma_{12}$  are increased by the presence of fibers.

## Discussion

### Viscosity

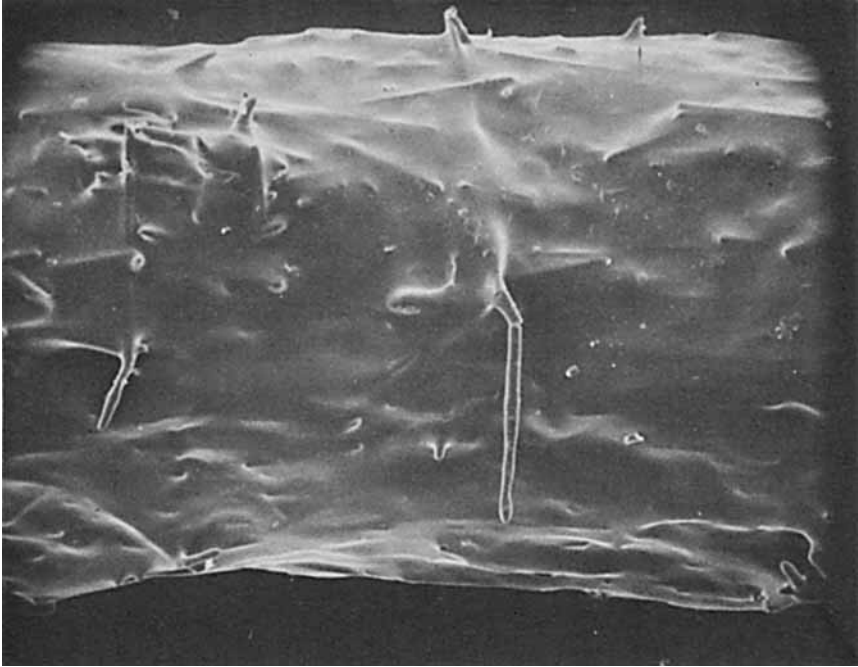
The viscosity–shear rate data for the pure polycarbonate melts are similar to that observed on other polycarbonate melts in the literature. The low shear rate Newtonian viscosity is similar in value to that reported for polycarbonates elsewhere in the literature<sup>17–19</sup> as well as unpublished studies in the LM Ericsson laboratories.

The viscosity–shear rate data from the cone-plate and capillary instruments agree, indicating that the viscosity of the fiber-reinforced melts is independent of instrument. This is in agreement with the observations of Chan, White, and Oyanagi,<sup>4</sup> and Charrier and Rieger<sup>2</sup> for fiber-filled polyolefins and polystyrene.

The viscosity data of the compounds appears to indicate a low shear rate Newtonian viscosity,  $\eta_0$ , as does the pure polycarbonate melt. While the  $\eta$ – $\dot{\gamma}$  slope of the composites decreases at low shear rates, it does not tend to zero slope. The glass fibers tend to make the melts less Newtonian. In terms of the power law

$$\eta = K\dot{\gamma}^{n-1} \quad (7)$$

the composite has values of order of 0.85 at low shear rates. Chan, White, and Oyanagi<sup>4</sup> and Czarnecki and White<sup>7</sup> found zero shear viscosities in their fiber-filled composites.

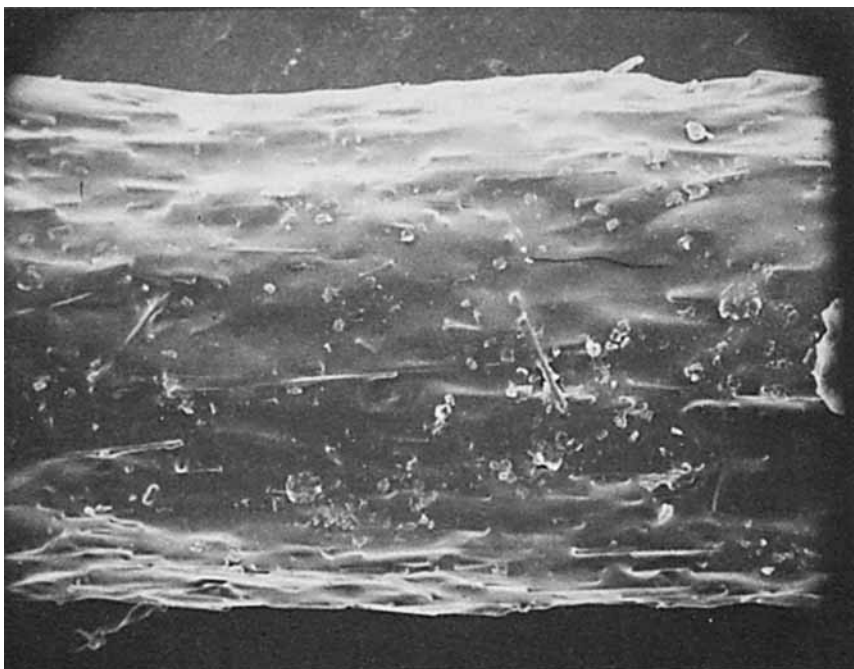


(a)



(b)

Fig. 11. SEM photomicrographs of 40% glass fiber/polycarbonate extrudates.  $\dot{\gamma}$ : (a), 19; (b), 192; (c), 1922 s<sup>-1</sup>.



(c)

Fig. 11. (Continued from previous page.)

Czarnecki and White<sup>7</sup> have shown that at low shear rates, Vinogradov and Malkin<sup>27</sup> reduced viscosity plots of  $\eta/\eta_0$  vs.  $\eta_0\dot{\gamma}$  may be applied to fiber-reinforced polystyrene melts. The reduced viscosity of the fiber-melt composite is the same function of  $\eta_0\dot{\gamma}$  as the melt matrix. This also may readily be shown to be valid for Chan, White, and Oyanagi<sup>4</sup> and Charrier and Rieger's<sup>2</sup> polyolefin data. We have found that it is difficult to select a zero shear viscosity for the polycarbonate glass fiber composites, and overlap throughout the entire shear rate region does not seem possible (see Fig. 4).

Some discussion of the ordering of the viscosity curves is needed. The failure of ordering of the data according to fiber content would appear to be due to a combination of breakdown of the fibers and degradation of the base polymer, both occurring during mixing. From our data it is seen that the fiber length has a large influence on the viscosity.

#### *Principal Normal Stress Difference*

We should first consider the principal normal stress difference for the polycarbonate melts and contrast it with the literature. We have not been able to locate any other normal stress data for polycarbonates. If one compares the  $N_1 - \sigma_{12}$  data for polycarbonate with that of polystyrene he finds the slope is much smaller and the magnitude is generally less than that for the commercial polystyrenes (PS) summarized by Oda, White, and Clark.<sup>26</sup> The magnitudes are closer to the monodisperse polystyrene, but the relative slope is much smaller. This is troubling because in a viscoelastic fluid in the Newtonian viscosity region, one expects  $N_1$  to be proportional to the square of  $\sigma_{12}$ , as predicted by Coleman and Markovitz.<sup>28</sup> The relatively narrow  $M_w/M_n$  of the polycarbonate would

lead one to expect data intermediate between the narrow molecular weight distribution samples and the commercial PS of Oda, White, and Clark.<sup>26</sup> Mechanistically, the more rigid backbone of polycarbonate as compared to PS could lead to different behavior but the comparison to the phenomenological theory is a problem.

The increase in the principal normal stress difference in the fiber-reinforced melts corresponds to the observation of Chan, White, and Oyanagi<sup>4</sup> and Czarnecki and White<sup>7</sup> in our laboratories. The data shown in Figure 3 closely resemble the plots of the latter authors in indicating an increase in  $N_1$  at fixed  $\sigma_{12}$  owing to the presence of the fibers. As mentioned by these authors, the increase in  $N_1$  seems to be a hydrodynamic particle effect, associated with the alignment of fibers along streamlines. It is well known that fibers cause Weissenberg effects in suspensions in Newtonian liquids.<sup>29,30</sup> We seem to have an additive or synergistic interaction between fibers and viscoelasticity.

## EXTRUSION

### Results

#### *Extrudate Swell*

The extrudate swell of the polycarbonate melt and its compounds is shown in Figure 5, as a function of die wall shear rate. The swell is reduced by the presence of the fibers.

#### *Fiber Orientation and Fiber Length Distribution*

From our studies of the surface fractures, we obtain the fiber orientation angle  $\theta$  to the streamline. In Figure 6, we plot the average fiber orientation, i.e., the fraction ( $H_{or}/H$ ) of the cross section which has oriented fibers versus die wall shear rate. Orientation gradually increases with extrusion of low rates but suddenly rises in the neighborhood of  $100 \text{ sec}^{-1}$ .

The fiber length distribution before and after extrusion is shown in Table II. The average length of the fibers is decreased on extrusion and the length distribution is narrowed.

#### *Surface Morphology*

In Figures 7–11 we show a range of SEM pictures of the surface at a series of different shear rates. The surface of the fiber-reinforced composites is significantly rougher under all conditions as compared to the polycarbonate, though the surface with the 30% concentration is smoother than the other composites. The *smoothness* of the extrudates increases with the extrusion rate.

### Discussion

The swell of the extrudates of the pure polycarbonate is not large. It is, however, completely suppressed by the addition of the glass fibers. This is in agreement with observations of earlier authors on other fiber-filled melts.<sup>3,5</sup>

The fiber orientation angle,  $\theta$ , appeared to be independent of the fiber loading level. The high orientation of the fibers developed during the flow through dies

is noteworthy. The rapid increase in orientation at about  $100 \text{ sec}^{-1}$  is not dissimilar to the observations of Wu.<sup>6</sup>

It is of interest that this orientation remains in the solidified filaments even without the application of tension to the emerging filaments. This helps explain the combined behavior of high normal stresses and low extrudate swell. The hydrodynamic effect of the fibers produce normal stresses. However, they do not disorient like macromolecules when exiting a die. In fact, they certainly inhibit the recovery of the matrix melt.

Fiber breakage is significant and is perhaps caused by the rotation of the fibers during flow as suggested by Czarnecki and White.<sup>7</sup> The fiber length distribution is narrowed during extrusion. The representation of this effect is, however, suppressed by using the polydispersity  $\bar{L}_w/\bar{L}_n$  instead of the standard deviation as a measure of the broadness of the distribution.

The surface of the fiber-reinforced extrudates is much rougher than of the pure polycarbonate. The compound containing 30% glass fibers has a much smoother surface owing to the very short fiber lengths. We note also that the higher the extrusion rate the smoother the surface. This is probably related to increased fiber orientation.

B. Anders Knuttson would like to thank the Marcus Wallenberg Foundation and Telefon AB LM Ericsson for financial support during his stay at the University. This research was supported in part by the National Science Foundation under Grant Eng. 76-/19815. We would also like to thank Bayer AG, Leverkusen, West Germany, for supplying the material used in this work. We would especially like to thank Mr. B. L. McGill for his help with the scanning electron microscope.

## References

1. D. P. Thomas and R. S. Haghan, Soc. Plastics Ind., Reinforced Plastics Div. Prepr., 3-C, 1966.
2. J. M. Charrier and J. M. Rieger, *Fibre Sci. Technol.*, **7**, 161 (1974).
3. Y. Oyanagi and Y. Yamaguchi, *J. Soc. Rheol. Jpn.*, **3**, 64 (1975).
4. Y. Chan, J. L. White, and Y. Oyanagi, *J. Rheol.*, **22**, 507 (1978).
5. Y. Chan, J. L. White, and Y. Oyanagi, *Polym. Eng. Sci.*, **18**, 268 (1978).
6. S. Wu, *Polym. Eng. Sci.*, **19**, 638 (1979).
7. L. Czarnecki and J. L. White, *J. Appl. Polym. Sci.*, **25**, 1217 (1980).
8. J. E. O'Connor, *Rubber Chem. Technol.*, **50**, 945 (1977).
9. M. W. Darlington and P. L. McGinley, *J. Mater. Sci.*, **10**, 910 (1975).
10. K. Yoshida, G. Budiman, Y. Okayama, and T. Kitao, *Sen i Gakkaishi*, T 225 (1975).
11. L. A. Goettler, R. I. Leib, and A. J. Lambright, *Rubber Chem. Technol.*, **52**, 838 (1979).
12. L. A. Goettler, *Mod. Plastics*, 140 (April 1970).
13. M. J. Owen, D. H. Thomas, and M. S. Found, *Mod. Plastics*, 61 (June 1978).
14. O. L. Forgacs and S. G. Mason, *J. Colloid Sci.*, **14**, 457 (1959).
15. K. N. Murty and G. F. Modlen, *Polym. Eng. Sci.*, **17**, 848 (1977).
16. E. Bartram, H. L. Goldsmith, and S. G. Mason, *Rheol. Acta*, **14**, 776 (1975).
17. G. F. Baumann and S. Steingiser, *J. Polym. Sci. Part A 1*, 3395 (1963).
18. M. Yamada and R. S. Porter, *J. Appl. Polym. Sci.*, **18**, 1711 (1974).
19. K. B. Abbas, *Polym. Eng. Sci.*, (Proc. 2nd Internat. Symp. Degradation and Stabilization of Polym., Dubrovnik Yugoslavia (1979)).
20. K. B. Abbas, private communication, 1979.
21. K. B. Abbas, *Polym. Prepr., Am. Chem. Soc. Div. Polym. Chem.*, **18**, (2), 231 (1977).
22. E. B. Bagley, *J. Appl. Phys.*, **28**, 624 (1957).
23. K. Walters, *Rheometry*, Chapman and Hall, London, 1975.
24. J. L. White and A. B. Metzner, *Trans. Soc. Rheol.*, **7**, 295 (1963).
25. C. D. Han, *Rheology in Polymer Processing*, Academic, New York, 1976.

26. K. Oda, J. L. White, and E. S. Clark, *Polym. Eng. Sci.*, **18**, 25 (1978).
27. G. V. Vinogradov and A. Y. Malkin, *J. Polym. Sci., Part A-2*, **4**, 135 (1966).
28. B. D. Coleman and H. Markovitz, *J. Appl. Phys.*, **35**, 1 (1964).
29. R. O. Maschmeyer and C. T. Hill, *Adv. Chem. Ser.*, **134**, 95 (1974).
30. J. Mewis and A. B. Metzner, *J. Fluid Mech.*, **62**, 593 (1974).

Received April 14, 1980

Accepted July 31, 1980

Manuscript complete March 31, 1981